Supporting Information

Spike Protein Fragments Promote Alzheimer's Amyloidogenesis

Sujian Cao,[1†] Zhiyuan Song,[2†] Jinyu Rong,[3†] Nicholas Andrikopoulos,[1,4] Xiufang Liang,[1,5] Yue Wang,[1,5] Guotao Peng,[3*] Feng Ding,[2*] Pu Chun Ke[1,4*]

[1]Nanomedicine Center, The Great Bay Area National Institute for Nanotechnology Innovation, 136 Kaiyuan Avenue, Guangzhou, 510700, China

[2]Department of Physics and Astronomy, Clemson University, Clemson, SC 29634, USA

[3]College of Environmental Science and Engineering, Tongji University, 1239 Siping Road, Shanghai 200092, China

[4]Drug Delivery, Disposition and Dynamics, Monash Institute of Pharmaceutical Sciences, Monash University, 381 Royal Parade, Parkville, VIC 3052, Australia

[5]School of Biomedical Sciences and Engineering, Guangzhou International Campus, South China University of Technology, Guangzhou, 510006, China

[†]These authors contributed equally.

Corresponding Authors

Email: Guotao Peng, guotaopeng@tongji.edu.cn; Feng Ding, fding@clemson.edu; Pu Chun Ke, pu-chun.ke@monash.edu.

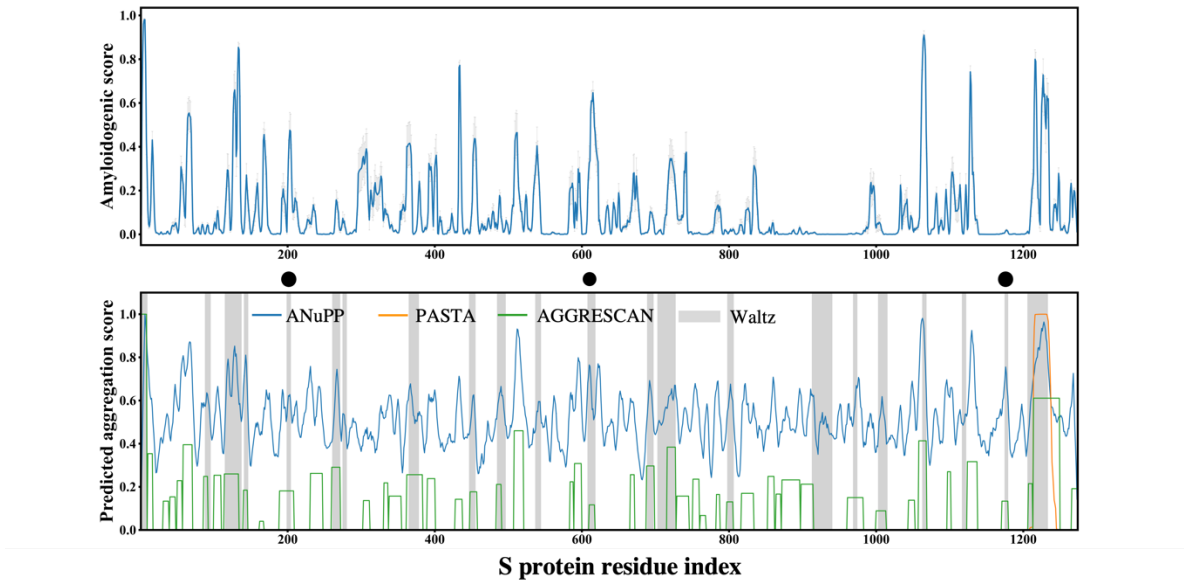

Fig. S1 Amyloidogenicity examination of spike protein using DMD and other popular predictors, including ANuPP, PASTA, AGGRESCAN, and Waltz. The amyloidogenic score, represented as a multiplication of average contact frequency between peptide residues and their β-sheet propensities, is depicted with error bars showing standard errors from ensemble averages over all independent trajectories. Spike protein fragments, indicated by black dots above the lower panel, were investigated and observed to undergo fibril formation in the study conducted by Sofie Nyström and Per Hammarström.[1]

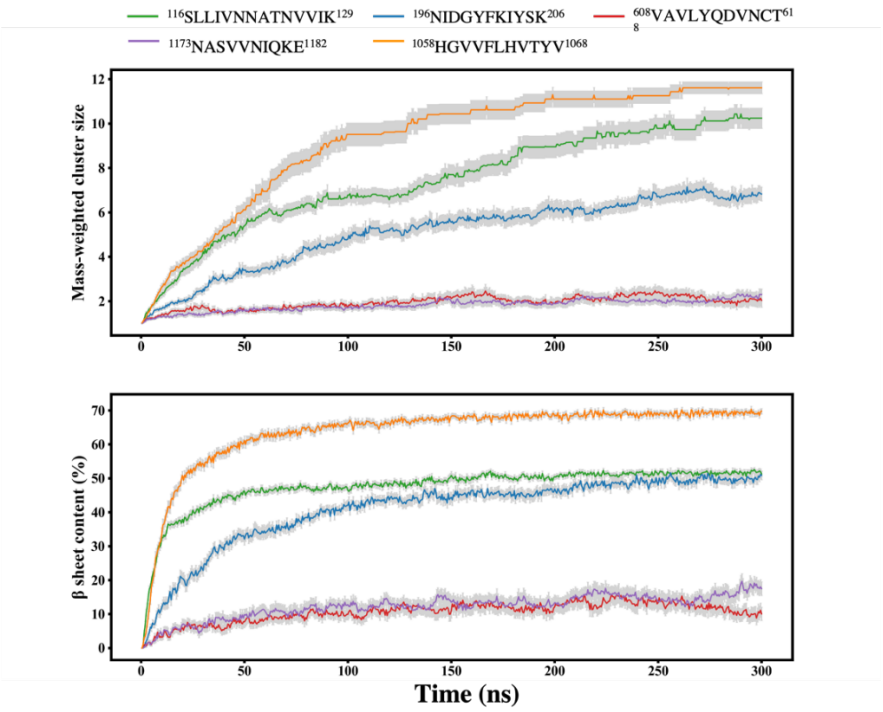

Fig. S2 Mass-weighted cluster size and β-sheet content per peptide of five targeted spike protein fragments are plotted over time. Error bars represent the standard error from the ensemble average across all independent trajectories.

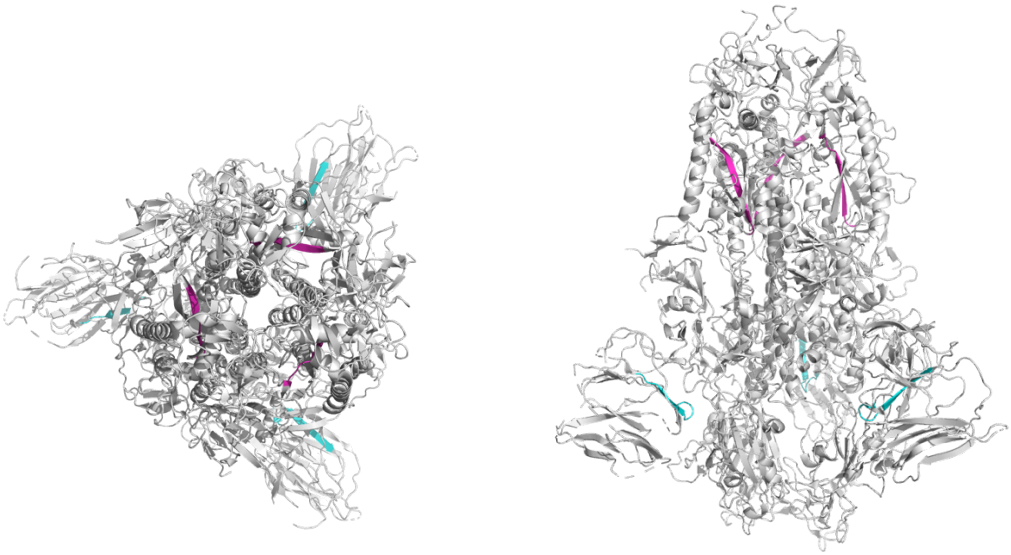

Fig. S3 Spike196 (cyan) and Spike1058 (red) shown in the full-length Spike protein trimer (PDB ID: 8H3D). The trimer is shown as cartoon and two different views are shown. Both fragments adopt β-sheet conformation in the folded state but are buried. Only upon proteolytic cleavage, these amyloidogenic peptide might be able to self-assemble into amyloid fibrils.

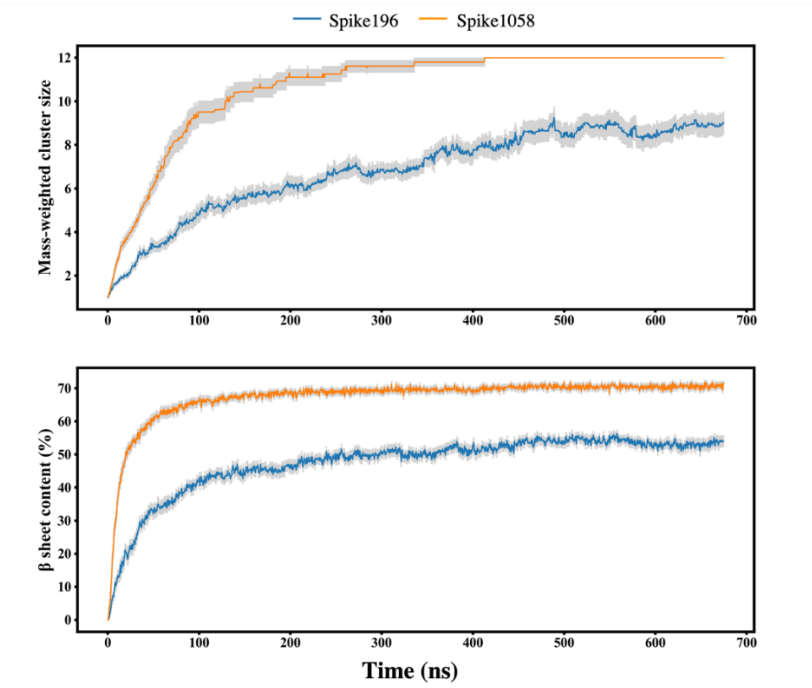

Fig. S4 Time evolution of mass-weighted cluster size and β-sheet content per peptide for Spike196 and Spike1058, two selected fragments, with extra 400 ns simulation time. Error bars represent the standard error from the ensemble average across all independent trajectories.

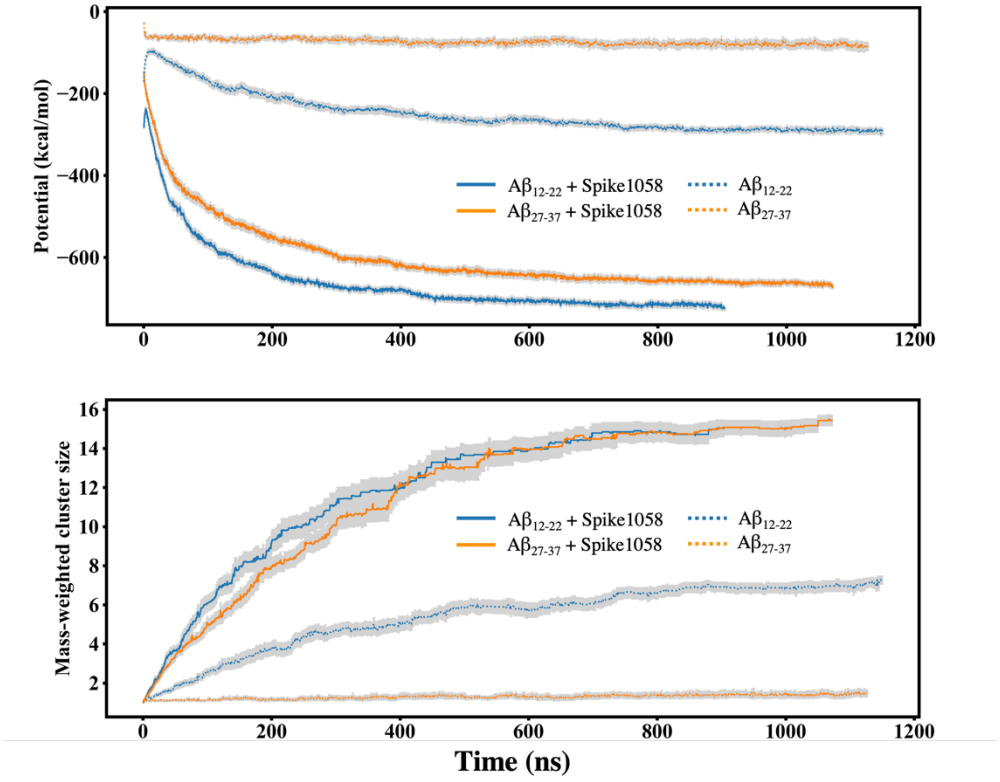

Fig. S5 Effect of addition of equal amount of Spike1058 on mass-weighted cluster size and potential energy of $A\beta_{12\text{-}22}$ and $A\beta_{27\text{-}37}$ is illustrated. Error bars indicate the standard errors from ensemble averages over all independent trajectories.

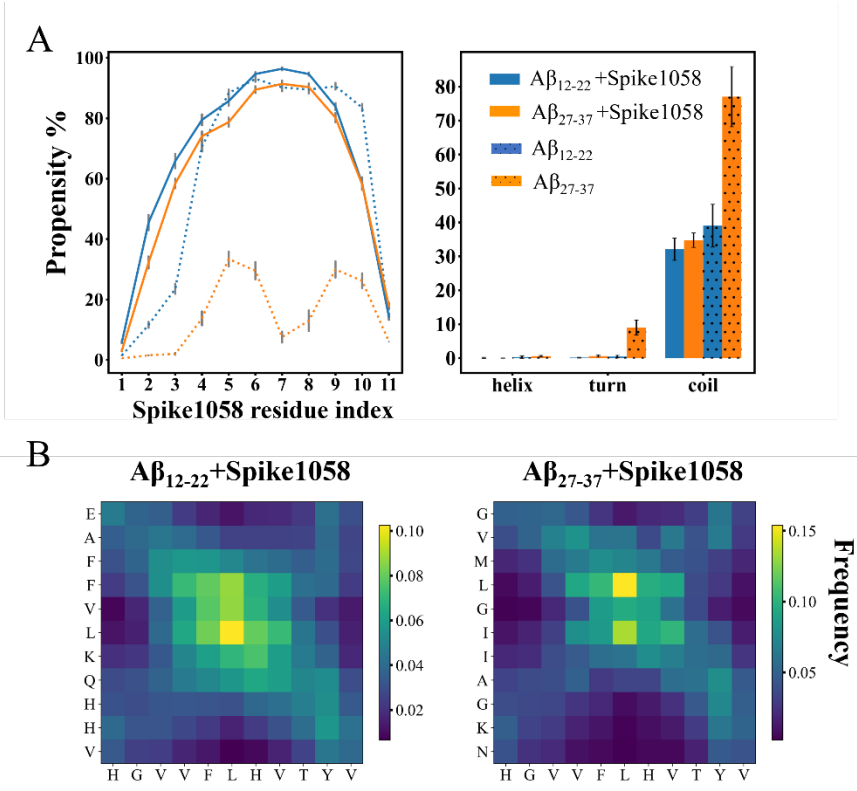

Fig. S6 A) Residue-wise β-sheet propensity per peptide and other secondary structure content per peptide during equilibrated simulations. B) Interpeptide contact maps of Aβ fragments with Spike1058 using the simulation results from static stage.

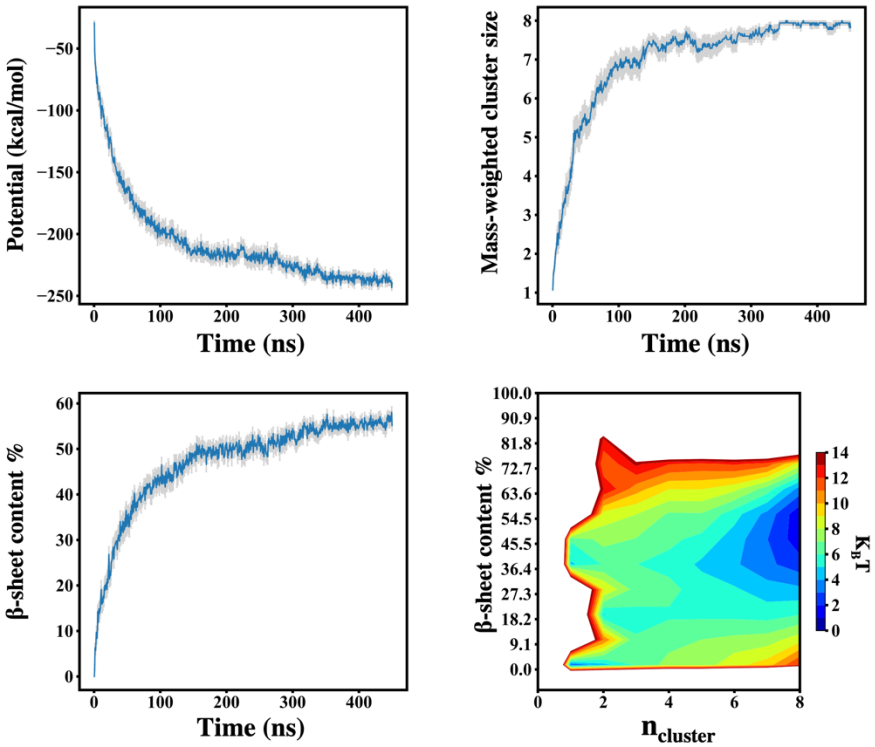

Fig. S7 Self-aggregation of Aβ$_{27-37}$. A smaller simulation box of 10 nm, compared to the 20 nm box (Method, aggregation simulations), was utilized to achieve a higher effective concentration of Aβ$_{27-37}$. The potential energy, mass-weighted cluster size, and β-sheet content per peptide as a function of time are presented. A 2D PMF for the aggregation free-energy landscape of Aβ$_{27-37}$ demonstrates the formation of aggregates with high β-sheet content, indicating the capability of Aβ$_{27-37}$ for self-aggregation.

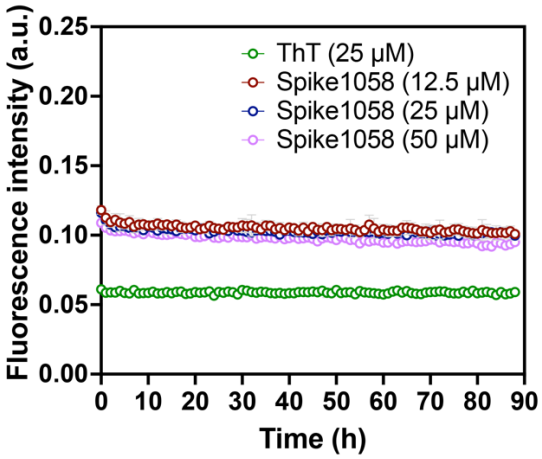

Fig. S8 ThT fluorescence assay of Spike1058 in a range of concentrations (12.5-50 μM) over time (0-90 h) in the presence of ThT dye (25 μM).

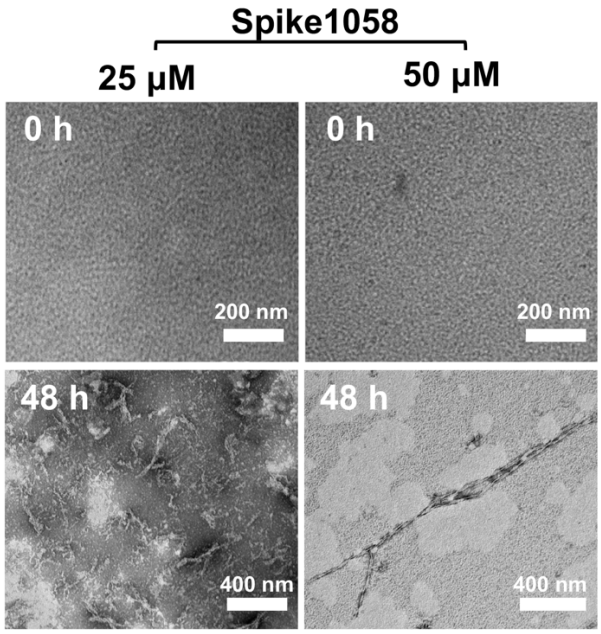

Fig. S9 TEM images of non-incubated (0 h) and incubated (48 h) Spike1058 at 25 and 50 μM.

Table. S1 HPLC analysis of $A\beta_{42}$ and Spike1058 co-aggregation.

37 ℃	$A\beta_{42}$		Spike1058	
	0 h	4 h	0 h	4 h
$A\beta_{42}$	100%	102.52%[a]	-	-
Spike1058	-	-	100%	98.54%[b]
$A\beta_{42}$ + Spike1058 (1:2)	100%	126%[c]	100%	60.46%[c]

*a: compared with $A\beta_{42}$ at 0 h; b: compared with Spike1058 at 0 h; c: compared with $A\beta_{42}$ + Spike1058 (1:2) at 0 h.

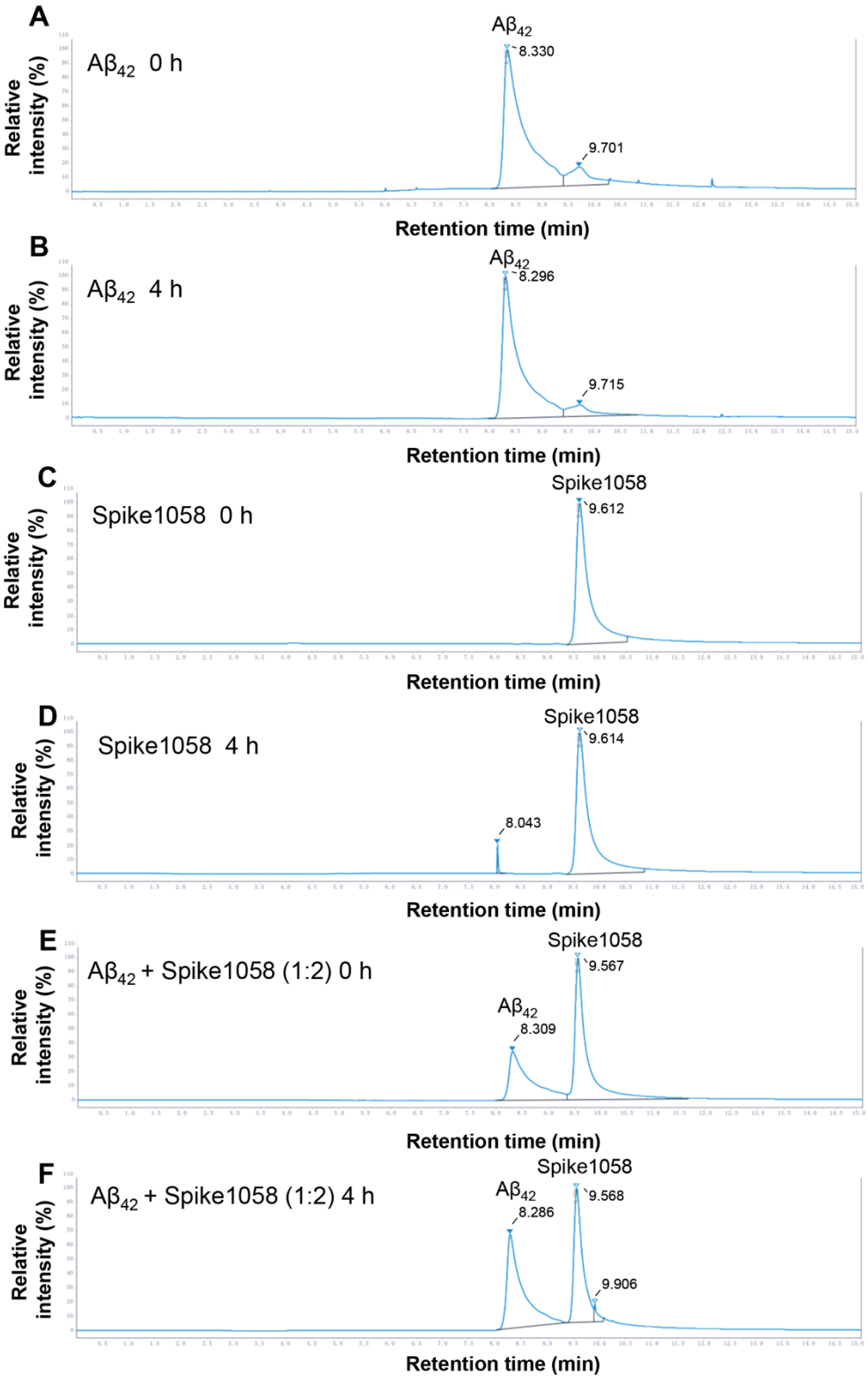

Fig. S10. HPLC chromatographs of non-incubated (0 h) (A) and incubated (4 h) (B) Aβ, non-incubated (0 h) (C) and incubated (4 h) (D) Spike1058, and non-incubated (0 h) (E) and incubated (4 h) (F) Aβ + Spike1058 at a 1:2 molar ratio. The numbers next to the peaks indicate the retention times.

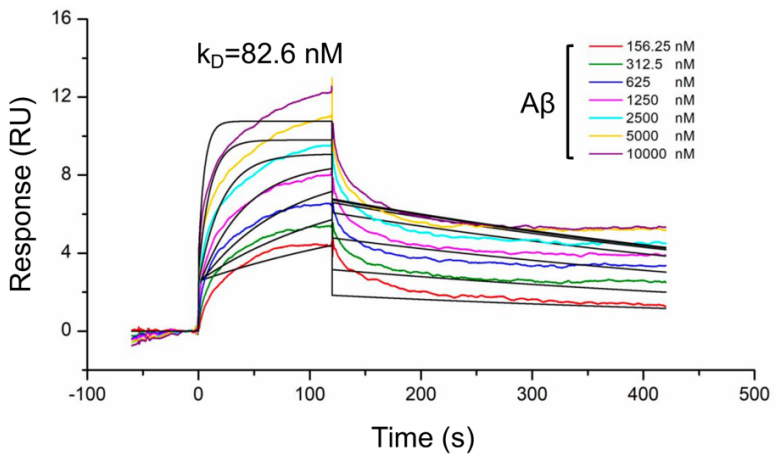

Fig. S11 Kinetics of Aβ binding affinity with Spike1058 as revealed by surface plasmon resonance (SPR) spectroscopy.

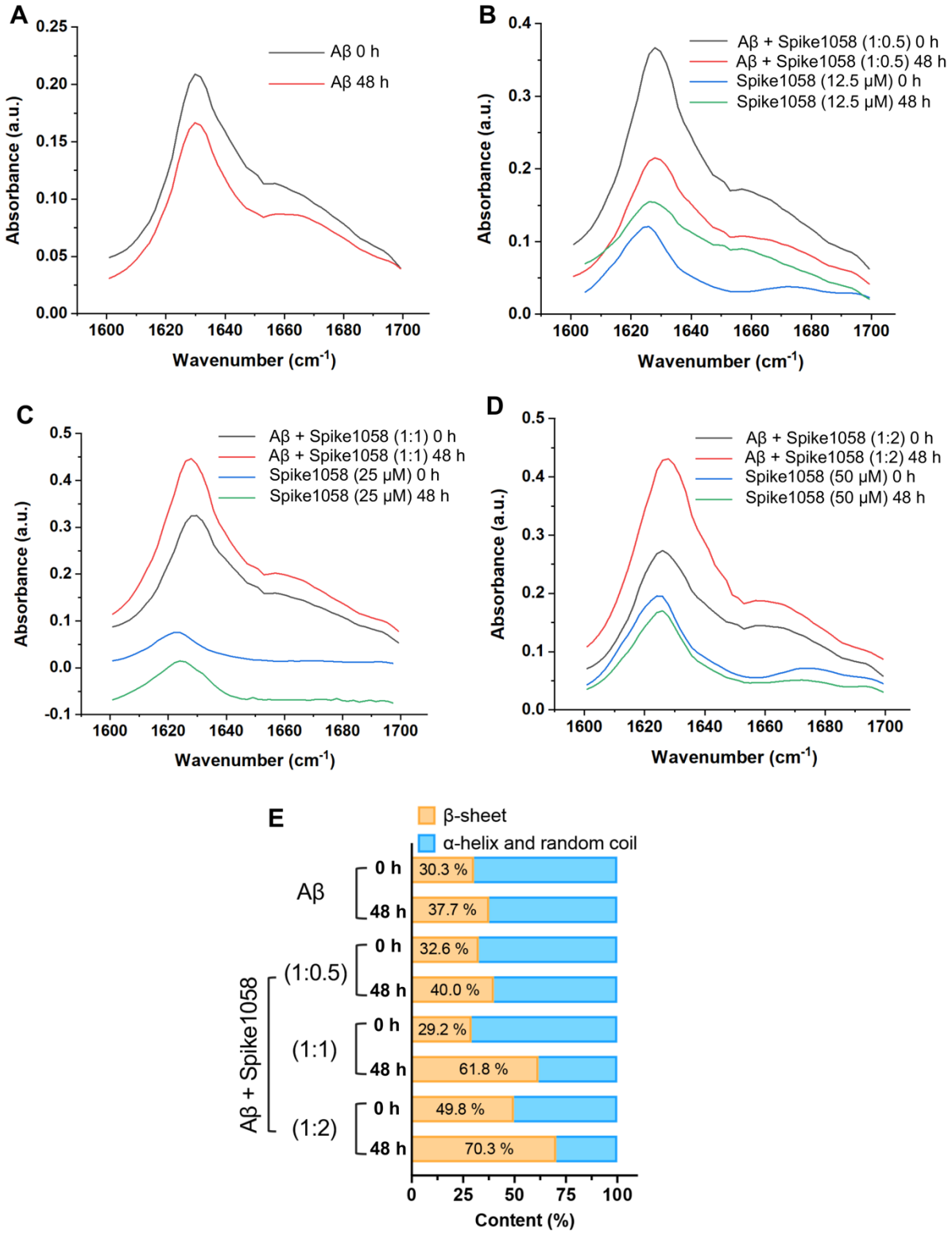

Fig. S12 Spike1058 accelerated Aβ fibrillization and the interaction between Spike1058 and Aβ. (a-d) FTIR spectra (1560-1725cm $^{-1}$) for non-incubated (0 h) and incubated (48 h) Aβ (25 μM) in the absence (a) and presence of 12.5 μM (b), 25 μM (c) and 50 μM Spike1058 (d). FTIR spectra of Spike1058 at their respective concentrations (12.5, 25 and 50 μM) were acquired as control. (e) Secondary structure contents inferred from the FTIR data.

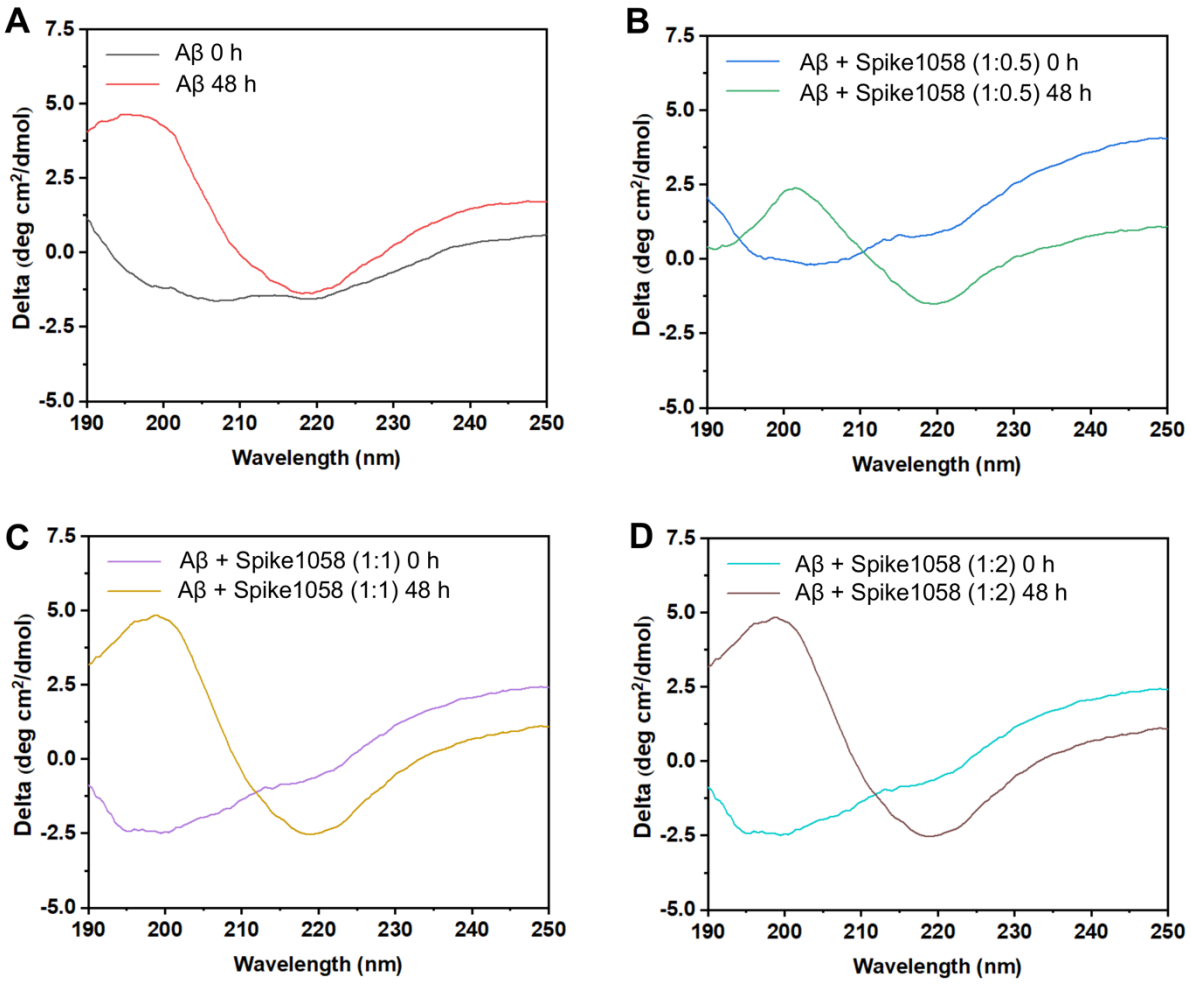

Fig. S13 CD spectra (190-250 nm) for non-incubated (0 h) and incubated (48 h) Aβ (25 μM) in the absence (a) and presence of 12.5 μM (b), 25 μM (c) and 50 μM (d) Spike1058.

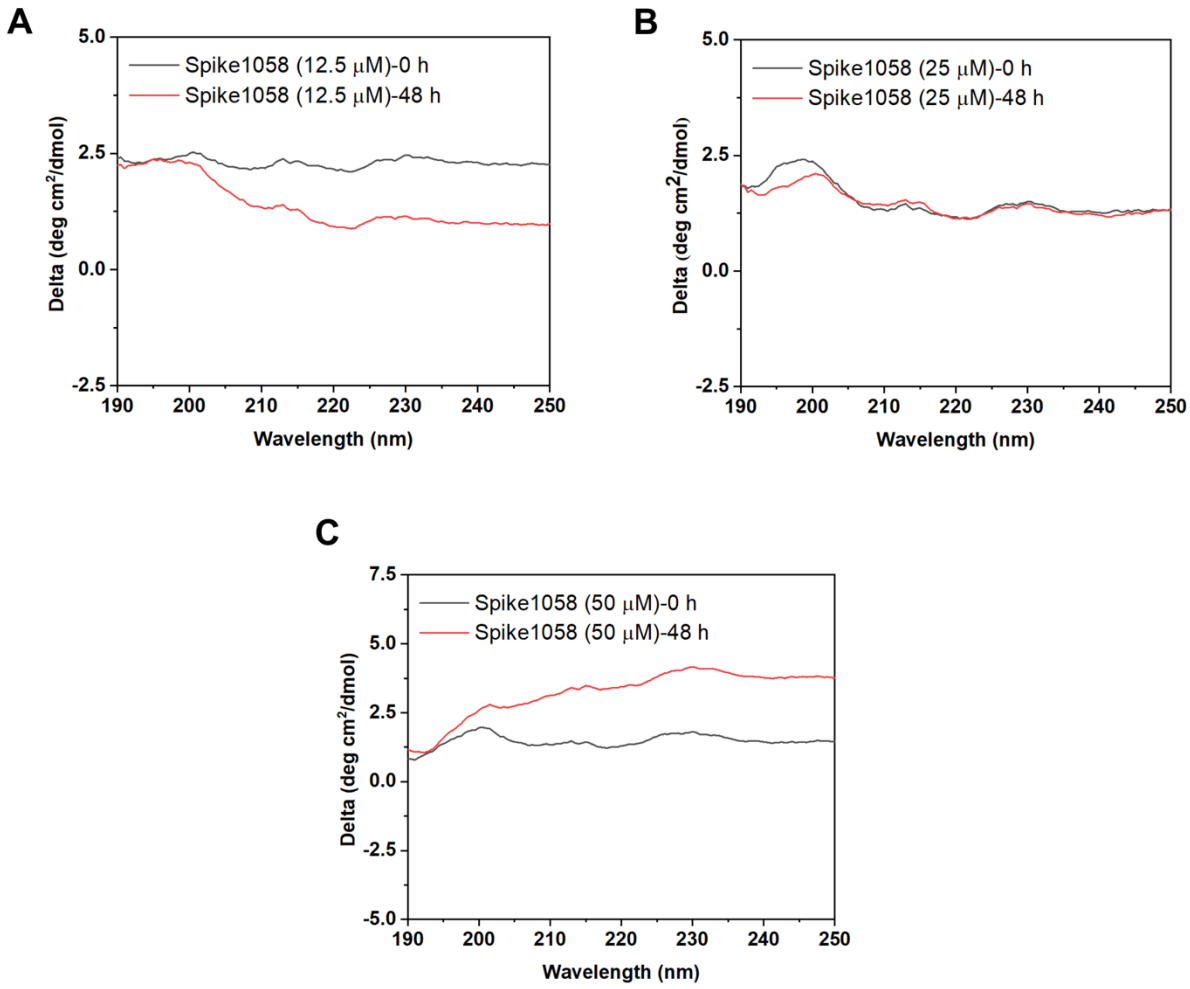

Fig. S14 CD spectra (190-250 nm) for non-incubated (0 h) and incubated (48 h) Spike1058 at concentration of 12.5 μM (a), 25 μM (b) and 50 μM (c), respectively.

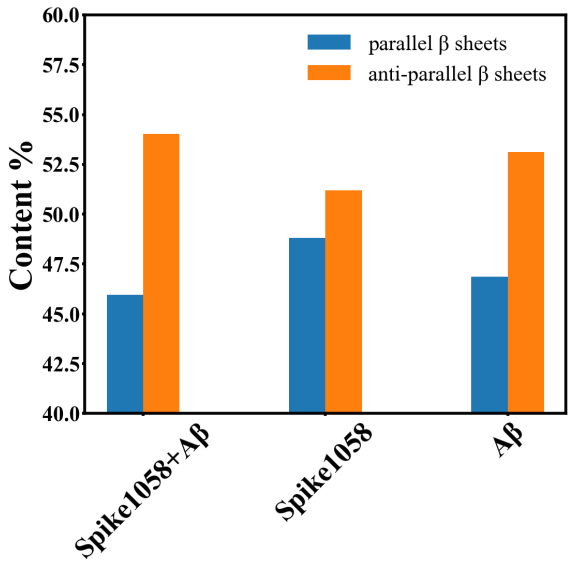

Fig. S15 Parallel and anti-parallel β sheet ratio for the co-aggregation of Spike1058 and Aβ as well as for the self-aggregation of Spike1058 and Aβ individually. In the simulations that included Aβ fragments, we calculated the average content of parallel and anti-parallel β sheets, taking into account of the 1:1 ratio of $A\beta_{12\text{-}22}$ and $A\beta_{27\text{-}37}$ fragments within an Aβ monomer. The results for all three scenarios are presented together.

References

1. Nystrom, S.; Hammarstrom, P. Amyloidogenesis of SARS-CoV-2 Spike Protein. *J Am Chem Soc* **2022,** *144*, 8945-8950.